

**BASE PRESSURE AND STATIC  
PRESSURE FOR A CONE-CYLINDER  
AT A NOMINAL MACH NUMBER OF 5.8**

---

**William D. Harkins**











BASE PRESSURE AND STATIC PRESSURE  
FOR A CONE-CYLINDER  
AT A NOMINAL MACH NUMBER OF 5.8

8854  
on spine:

HARKINS

1954

THESIS  
H23

Letter on front cover:

BASE PRESSURE AND STATIC PRESSURE  
FOR A CONE-CYLINDER AT A NOMINAL  
MACH NUMBER OF 5.8

William D. Harkins





Thesis by  
William D. Harkins  
" "  
Lieutenant, U. S. Navy

In Partial Fulfillment of the Requirements  
For the Degree of  
Aeronautical Engineer

California Institute of Technology  
Pasadena, California

1954

Thesis  
H23

## ACKNOWLEDGMENTS

The author wishes to express his gratitude and appreciation to Dr. H. T. Nagamatsu for his supervision, guidance, personal interest, and helpful suggestions; and to Mrs. H. Van Gieson for her assistance in the careful preparation of the manuscript.



## ABSTRACT

An experimental investigation was made in the GALCIT Hypersonic Wind Tunnel Leg No. 1 to determine the base pressure and static pressure on a cone-cylinder at a nominal Mach number of 5.8 in both one-phase and two-phase flow.

The scope of the investigation was a determination of interference data necessary for proper evaluation of base pressure results, investigation of the effect of Reynolds number on base pressure, and a comparison of experimental and theoretical static pressure distribution on a cone-cylinder.

As has been noted by other investigators, viscous effects in hypersonic flow were quite pronounced and demonstrated the increased non-linearity of the problems in hypersonic flow.



# TABLE OF CONTENTS

PART	TITLE	PAGE
	Acknowledgments	ii
	Abstract	iii
	Table of Contents	iv
I.	Introduction	1
II.	Experimental Equipment and Procedure	
	A. Description of the Wind Tunnel and Instrumentation	3
	B. Description of the Models	4
	C. Test Procedure	6
	1. Interference Data	6
	2. Base Pressure Data	7
	3. Static Pressure Data	8
III.	Discussion of Results	9
	A. *Sting Interference Investigation	9
	1. Critical Length of Sting	9
	2. Sting Diameter	9
	B. Variation of Base Pressure with Reynolds Number	11
	C. Static Pressure Distribution	13
V.	Conclusions	15
	References	16
	List of Figures	18
	Figures	19





## I. INTRODUCTION

In supersonic and hypersonic flight, it has been found that base drag contributes a large portion of the drag experienced by the body. Since only limited data seems to be available on base pressure in the hypersonic speed range, an investigation in this field was undertaken. In addition, it was desired to obtain some static pressure data in which condensation of the constituents of the air was a factor. It can be easily seen that a hypersonic wind tunnel cannot reproduce exactly ambient conditions experienced in flight. Large expansion ratios lead directly to low ambient temperatures in the test section -- much lower, in fact, than ambient temperatures experienced at high altitudes. In previous investigations, the stagnation temperature was raised to as high a level as practicable so that the test section static temperature would not be low enough to permit condensation. However, an increase in the Mach number corresponds to a larger expansion ratio, which in turn means an increase in the temperature drop to static test section conditions. It can be appreciated that the alternatives possible at higher Mach numbers for a wind tunnel using air are as follows:

- (1) Development of new materials and cooling to withstand very high stagnation temperatures
- (2) Analysis of data with condensation present

The investigation of the effects of condensation of air upon the aerodynamic characteristics at high Mach numbers has been discussed in Refs. 8 and 9. In undertaking the collection of static pressure data with and without condensation (also called two-phase and one-phase flow), no attempt was made to formulate any theories. It was desired



to obtain the information so that it would be available to future investigators.

All work was done at a nominal Mach number of 5.8 in Leg No. 1 of the GALCIT Hypersonic Wind Tunnel. However, the design and materials used in the models were chosen so that they might be used without modification in Leg No. 2 at a Mach number of approximately 10.

Before any base pressure determination could be made, it was necessary to obtain interference data at the test Mach number of 5.8. Chapman, in Ref. 1, has specifically stated the need for such interference data at the higher Mach numbers. Briefly, the data was obtained by various combinations of sting and side support of the models. The various ramifications of this problem will be discussed at greater length in the appropriate section.



## II. EXPERIMENTAL EQUIPMENT AND PROCEDURE

### A. Description of the Wind Tunnel and Instrumentation

All testing was carried out in the GALCIT 5" x 5" Hypersonic Wind Tunnel (Log No. 1), which is of the continuously-operating, closed-return type. The required compression ratios were obtained with five stages of Fuller rotary compressors, and, when necessary, an additional stage of Ingersoll reciprocating compressors. The compressors and all the valving were operated remotely from a master control panel located adjacent to the test section. The air heating system consisted of a multiple-pass heat exchanger with superheated steam as the heating medium. The capacity of the system was such that a stagnation temperature of 300°F was obtainable at a stagnation pressure of 94.9 psia.

Oil removal was accomplished by cyclone separators after each compression stage, finely-divided carbon canisters, porous carbon filter blocks, and a fibre glass filter. The air used during the tests contained approximately 2.5 parts per million (ppm) of oil fog by weight.

Water was removed by a 2200-pound bed of silica gel in the main air circuit, which was reactivated by an integral blower-heater-condenser system prior to each run. The maximum water content of the air was kept below 100 ppm by weight at all times, the usual content being approximately 22 ppm.

The tests were conducted at a nominal Mach number of 5.8. The nozzle blocks were designed by the Foelsch method with correction applied for the estimated boundary layer displacement thickness. Static orifices at one-inch intervals in the top and bottom nozzle blocks





permitted a check with the original nozzle calibration to be made during each run. The results of independent static pressure surveys were utilized to determine axial static pressure variation in the test rhombus. These tests indicated a negligible variation in the section used, and thus obviated any correction for this effect.

A 32-tube vacuum-referenced manometer using DC-200 silicone fluid was used to measure all static pressures. Tunnel stagnation pressure was measured with a Tate-Emery nitrogen-balanced gage, and this pressure was controlled within  $\pm 0.04$  psi by means of a Minneapolis-Honeywell-Brown circular chart controller.

The stagnation temperature was measured by a thermocouple probe located one inch upstream from the nozzle throat. This temperature was recorded and controlled by means of a Minneapolis-Honeywell-Brown circular chart controller. All other temperatures necessary for plant operation were indicated on a 20-point Leeds and Northrup recorder.

An optical system using a BH-6 steady source was used for the schlieren photographs of the flow.

## B. Description of the Models

In this investigation, three models of basic cone-cylinder configuration were used. All models were constructed of stainless steel, with silver solder where necessary, thus enabling their use in Leg No. 2 of the Hypersonic Wind Tunnel as well as Leg No. 1.

The models shown in Figs. 1, 2, and 4 were used for the determination of interference data and base pressure data. The shrouds used for the tests were slipped over the sting when needed. Dimensions for the shrouds were  $d/h = 0.5, 0.75, 0.875, \text{ and } 1.0$ . The model shown in





Figs. 3 and 5 was used for the determination of static pressure in one-phase and two-phase flow.

The basic  $L/D$  of the cone-cylinder combination was chosen to be the same as the one discussed in Ref. 1 to facilitate possible comparison of the data. The sting diameter was slightly larger than was desirable. However, availability and preliminary structural calculations dictated the particular choice. On the basis of previous investigations, it was felt that sting length would affect the tests to a greater extent than sting diameter.

Since a central body support was not available in the tunnel, a modified rear support system was utilized (Fig. 6). Rear support rods were fitted with two collars, the upstream collar being a cone-cylinder combination, and the sting went through the collars. Set screws in the collars were used to maintain the lateral position of the model.

For the tests requiring a side support, a modified double wedge airfoil section was used. This airfoil was silver soldered to a block which was held in a standard insert block on the floor of the tunnel (Fig. 7). The size of the airfoil was determined as the optimum which would allow certain features of the design assembly to be incorporated without undue difficulty of machining and which would probably, on the basis of other results, produce no undesirable aerodynamic effects.

All threaded surfaces were copper plated with the idea that it would not be necessary to unscrew any parts after having once seated the threads, thereby avoiding leakage around the threads. Subsequent leak tests showed the necessity of coating the threaded surfaces with Glyptal to prevent leakage. The inside of the model shown in Fig. 3 was filled with Sauereisen cement to provide support for the static pressure lines.



## C. Test Procedure

### 1. Interference Data

The model shown in Fig. 1 was sting supported with a  $d/h = 0.3125$ . The support length from the model base to the upstream tip of the first collar was varied from four inches to eight inches in increments of one inch. The test was conducted under the following conditions:  $T_o = 280^\circ\text{F.}$ ,  $p_o = 32.6$  psig,  $Re = 620000$  (based upon the model length). This pressure was used in order to decrease the response time necessary during the tests to obtain an estimate of the critical length. Although it was desirable to repeat the test at a lower pressure, subsequent tests showed that the response time would be so great as to make this unfeasible with the present system. Therefore, the tests at lower pressures were not made.

As in Ref. 11, the critical sting length is defined as the minimum sting length possible for obtaining a base pressure which is 0.5% of that obtained with an "infinite" length sting. Also, as in Ref. 11, the critical sting length decreases monotonically with increasing Reynolds number. Therefore, with the method used, no "feed-up" from the support would be encountered in subsequent tests if the sting length were fixed as satisfying the most critical conditions, namely, the lowest Reynolds number.

The critical sting length having been determined, it was desirable to study the effect of variation of support diameter. For this, the model was sting supported for the various runs. Shrouds were merely slipped over the sting to vary  $d/h$  thus:  $d/h = 0.3125, 0.5, 0.75, 0.875, 1.0$ .



The runs were as follows:

$T_o(^{\circ}F.)$	$p_o(\text{psig})$	$Re \times 10^{-5}$
225	32.6	6.89
150	80	17.2

It should be noted that the first run was with one-phase flow, while the second run was with two-phase flow.

## 2. Base Pressure Data

For the determination of base pressure data, the model was sting supported and side supported with and without the dummy sting for the various runs. For a constant  $d/h = 0.3125$ , the following test runs were conducted:

$T_o(^{\circ}F.)$	$p_o(\text{psig})$	$Re \times 10^{-5}$
280	80	12.4
280	32.6	6.20
280	10	3.23
225	80	14.0
225	32.6	6.89
225	10	3.65
190	80	15.32
150	80	17.2





### 3. Static Pressure Data

With the sting supported model as shown in Fig. 3, tests were conducted in one-phase and two-phase flow as follows:

$T_o(^{\circ}F.)$	$p_o(\text{psig})$	$Re \times 10^{-5}$
225	80	14.0
225	32.6	6.89
225	10	3.65
150	80	17.2

It should be noted that the two forward orifices in the model shown in Fig. 3 are symmetrical about the axis and were used to assure a zero angle of attack for the model in the test section flow.

Schlieren photographs taken during the tests are shown in Figs. 8 and 9.





### III. DISCUSSION OF RESULTS

#### A. Sting Interference Investigation

##### 1. Critical Length of Sting

The first tests were made to determine the "critical length" of the sting. Although, in the light of Ref. 11, it was desirable to run at the lowest available Reynolds number, an intermediate Reynolds number involving a  $p_0 = 32.6$  psig was run first. Even with this total pressure, response time was approximately thirty minutes for each point determined. On this basis, it was determined that it would be difficult with the present instrumentation to run at the lowest Reynolds number, requiring a  $p_0 = 1$  psig. The results of these tests are shown on Fig. 10. Interference from the rear support on the base pressure was found to be apparently non-existent for a sting length greater than seven inches. On the basis of this information, sting shrouds 7.5 inches in length were constructed for further determination of interference data. Base pressure measurements were taken on an Alphatron vacuum gage. However, the range of existing pressures was too high to utilize the Alphatron to the fullest advantage that would be possible if pressures were of the order of microns of mercury. Therefore, it was determined that subsequent pressure measurements would be taken on the silicone manometer.

##### 2. Sting Diameter

In the second series of tests the sting diameter was varied to determine the effect on base pressure. For this study, shrouds of  $d/h = 0.5, 0.75, 0.875$ , and  $1.0$  were used to fit over the original



sting. Base pressure measurements were taken in one-phase ( $T_o = 225^\circ\text{F.}$ ,  $p_o = 32.6$  psig) and two-phase ( $T_o = 150^\circ\text{F.}$ ,  $p_o = 80$  psig) flow. As stated previously, in taking these and all subsequent measurements the silicone manometer was utilized. The results of these tests are shown on Fig. 11. The two-phase flow showed rather conclusively that the original sting  $d/h$  was small enough to make reasonable the assumption of an absence of interference from the sting diameter. The evidence was not so conclusive in the case of the one-phase flow. The data shown was substantiated by subsequent runs. However, due to material availability limitations, it was not possible to determine an intermediate point of  $d/h$  between 0.3125 and 0.5. Therefore, the shape of the curve in this region could not be determined precisely.

It has been stated in Ref. 6 that there should be a slight increase in the negative amount of base pressure upon increasing the sting diameter beyond  $d/h = 0.1$ . Later tests by Chapman indicate that the permissible ratio is higher than 0.1. Unfortunately, due to experimental limitations, no results of the present tests are conclusive as to the validity of an actual criterion in this Mach range.

Reference 2 shows that, for Mach numbers greater than about 3, a monotonic decrease in the absolute value of the base pressure coefficient can be expected with an increase in support diameter. This conclusion was not substantiated in these tests.

Finally, for structural reasons, the minimum permissible  $d/h$  was 0.3125 in these tests, and we are forced to the conclusion that if any interference effect is present, it is small. Thus, the results of any future tests would have an uncertainty to the extent of this possible error.





## B. Variation of Base Pressure with Reynolds Number

The base pressure coefficient was defined as

$$C_p = \frac{P - P_\infty}{\frac{\gamma}{2} P_\infty M_\infty^2}$$

In the reduction of data, a nominal Mach number of 5.8 was used. This was chosen as representing an average value and obviated the difficulty of describing a Mach number in two-phase flow.

The third series of tests was to determine the variation in base pressure with Reynolds number. Toward this end, tests were conducted with the following model configurations:

- (1) Sting support alone ( $d/h = 0.3125$ ,  $l/h = 7.5$ )
- (2) Side support along
- (3) Side support with dummy sting ( $d/h = 0.3125$ ,  $l/h = 7.5$ )

The results of these tests are plotted as Fig. 12. Comparing the results from the model configuration (2) with those of (3), the added effect of the sting was determined. This was applied as a correction to results from the model configuration (1) to obtain the final curve. It can be seen that the variation of base pressure with Reynolds number is comparatively small in the particular range of Reynolds numbers attained. However, as was found at lower Mach numbers (Ref. 3), the variation is monotonic with increasing Reynolds number.

It has been stated in Ref. 3 that thin streamlined airfoils mounted on the body have little or no effect on base pressure. Since the side support used in the present tests conformed to the requirement of a thin streamlined airfoil, it would appear that the conclusion



drawn in Ref. 3 must be modified somewhat for the range of Mach and Reynolds numbers used during these tests. The use of the side support apparently did affect the base pressure considerably, and it would appear that the large viscous effects in the hypersonic range would probably account for this variance.

The tests conducted in two-phase flow presented some special difficulties. Naturally, a question as to the proper Reynolds number arose. Since at present there does not seem to be an accepted definition of effective Reynolds number when condensation is present, the Reynolds number based on the model length was calculated from the viscosity data as presented in Ref. 15. With the use of this definition of Reynolds number, it was found that the base pressure was greater in absolute value with all model configurations used than would reasonably be expected by an extension of the curve obtained in one-phase flow. As condensation occurs, velocity and density remain practically unaltered, while pressure and temperature are greater than that with an uncondensed flow as discussed in Refs. 8 and 9, and boundary layer thickness is reduced. Thus, the effect on base pressure in the present tests would seem to substantiate the theory propounded in Refs. 8 and 9 that condensation is increased after an expansion. In this case, as the flow expanded around the base of the model, more constituents of the air condensed, thus increasing the temperature and increasing the absolute base pressure, while decreasing the absolute value of the base pressure coefficient.





### C. Static Pressure Distribution

The final series of tests was to determine static pressure on a cone-cylinder in one-phase and two-phase flow. The results are shown as Fig. 13. Several interesting trends were noticed. Over the cone surface, the pressure was higher nearest the vertex than at other points on the cone. This phenomenon has also been observed on wedges in hypersonic flow, and it has been postulated as being due to an interaction between the shock wave and the boundary layer. The pressure on the cone in two-phase flow seemed to substantiate the theory given in Ref. 9. Since the flow passed through a conical shock at the nose of the cone, this shock decreased the flow condensation with a resultant decrease in absolute static pressure. While still discussing the two-phase flow, the static pressure on the cylinder might well be mentioned. The flow expanded around the shoulder which joined the cone and the cylinder, thus causing more constituents to condense while reducing the boundary layer thickness. These two effects tended to compensate for any net pressure change. The increased condensation tended to increase the absolute static pressure, while the decreased boundary layer thickness made the effective body radius smaller, thus permitting greater expansion and a lower absolute static pressure.

With regard to the variation of static pressure over the cylinder in one-phase flow, some interesting results are apparent. Potential theory shows that the static pressure ratio should reach some minimum value at the shoulder and then approach the free stream condition asymptotically. As determined experimentally, the static pressure



remained essentially constant at the highest Reynolds number used, and at the lower Reynolds numbers, static pressure actually decreased along the cylinder. This effect was also noticed in Ref. 14. The phenomenon appeared to be due to the viscous effects. As the stagnation pressure decreased, boundary layer growth increased. The increased boundary layer changed the effective shape of the body at the shoulder and resulted in a marked deviation from the theoretical value. To determine the theoretical values, a mean Mach number was chosen as shown. The pressure distribution over the cone was calculated from Ref. 12, and the distribution over the cylinder was calculated by the method of characteristics in axially-symmetric flow as given in Procedure IA of Ref. 13.



## V. CONCLUSIONS

The following conclusions, based upon the results of these tests in the GAIT 5" x 5" Hypersonic Wind Tunnel (Leg No. 1), appear valid:

(1) The critical length of the sting required to prevent feed-up in the boundary layer is approximately seven inches for the present test conditions,  $d/h = 0.3125$ .

(2) The effect of varying effective sting diameter is not a monotonic variation at a Mach number of 5.8.

(3) Base pressure increases monotonically for the Reynolds number range tested.

(4) The effect of viscosity is great enough to change the effective shape of the body in the vicinity of the shoulder and thus cause a noticeable deviation from the theoretical value in the region just behind the shoulder.





## REFERENCES

1. Chapman, Dean R. and Perkins, Edward W.: Experimental Investigations of the Effects of Viscosity on the Drag of Bodies of Revolution at a Mach Number of 1.5, NACA RM A7A31a, April 3, 1947.
2. Chapman, Dean R.: Base Pressure at Supersonic Velocities, California Institute of Technology, Ph.D. Thesis, 1948.
3. Hill, Freeman K. and Alpher, Ralph A.: Base Pressures at Supersonic Velocities, Jour. Ae. Sci., March 1949, pp. 153-160.
4. Chapman, Dean R.: An Analysis of Base Pressure at Supersonic Velocities and Comparison with Experiment, NACA TN 2137, July 1950.
5. Chapman, Dean R.: Note on Base Pressure Measurements, Jour. Ae. Sci., Dec. 1950, pp. 812-813.
6. Hoerner, Sigward F.: Base Drag and Thick Trailing Edges, Jour. Ae. Sci., Oct. 1950, pp. 622-628.
7. Potter, J. L.: Base Pressures at Supersonic Speeds, Jour. Ae. Sci., Feb. 1951, pp. 141-142.
8. Buhler, Rolf D. and Naganatsu, H. T.: Condensation of Air Components in Hypersonic Wind Tunnels -- Theoretical Calculations and Comparison with Experiment, California Institute of Technology, Guggenheim Aeronautical Laboratory, Hypersonic Wind Tunnel Memorandum No. 13, 1952.
9. Grey, J. and Naganatsu, H. T.: The Effects of Air Condensation on Properties of Flow and Their Measurement in Hypersonic Wind Tunnels, California Institute of Technology, Guggenheim Aeronautical Laboratory, Hypersonic Wind Tunnel Memorandum No. 8, 1952.
10. Mackay, Douglas S. and Naganatsu, H. T.: Boundary Layer Temperature Recovery Factor on a Cone at Nominal Mach Number Six, California Institute of Technology, Guggenheim Aeronautical Laboratory, Hypersonic Wind Tunnel Memorandum No. 15, 1953.
11. Kavanau, L. L.: Results of Some Base Pressure Experiments at Intermediate Reynolds Numbers with  $M = 2.84$ , Univ. of Calif. Report No. HE-150-117, Oct. 22, 1953.
12. Kopal, Zdenek: Tables of Supersonic Flow Around Cones, Mass. Institute of Technology, Technical Report No. 1, 1947.





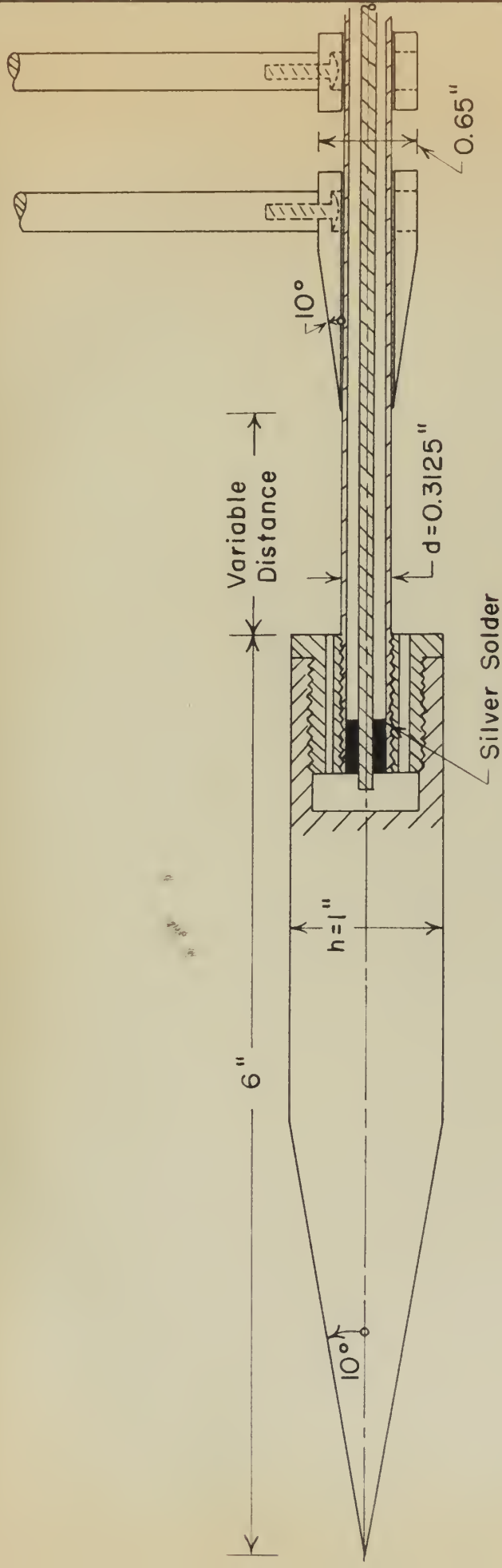
13. Isenberg, J. S.: The Method of Characteristics in Compressible Flow, Part I, Steady Supersonic Flow. Part IA, Tables and Charts. Part IB, Numerical Examples, U. S. Air Force Technical Report No. F-TR-1173A, B, C-ND, 1947.
14. McLellan, Charles H.: Exploratory Wind Tunnel Investigation of Wings and Bodies at  $M = 6.9$ , Jour. Ae. Sci., Oct. 1951, pp. 641-648.
15. Table 2.39 - Dry Air - Coefficients of Viscosity, The NBS-NACA Tables of Thermal Properties of Gases, Dec. 1950.



## LIST OF FIGURES

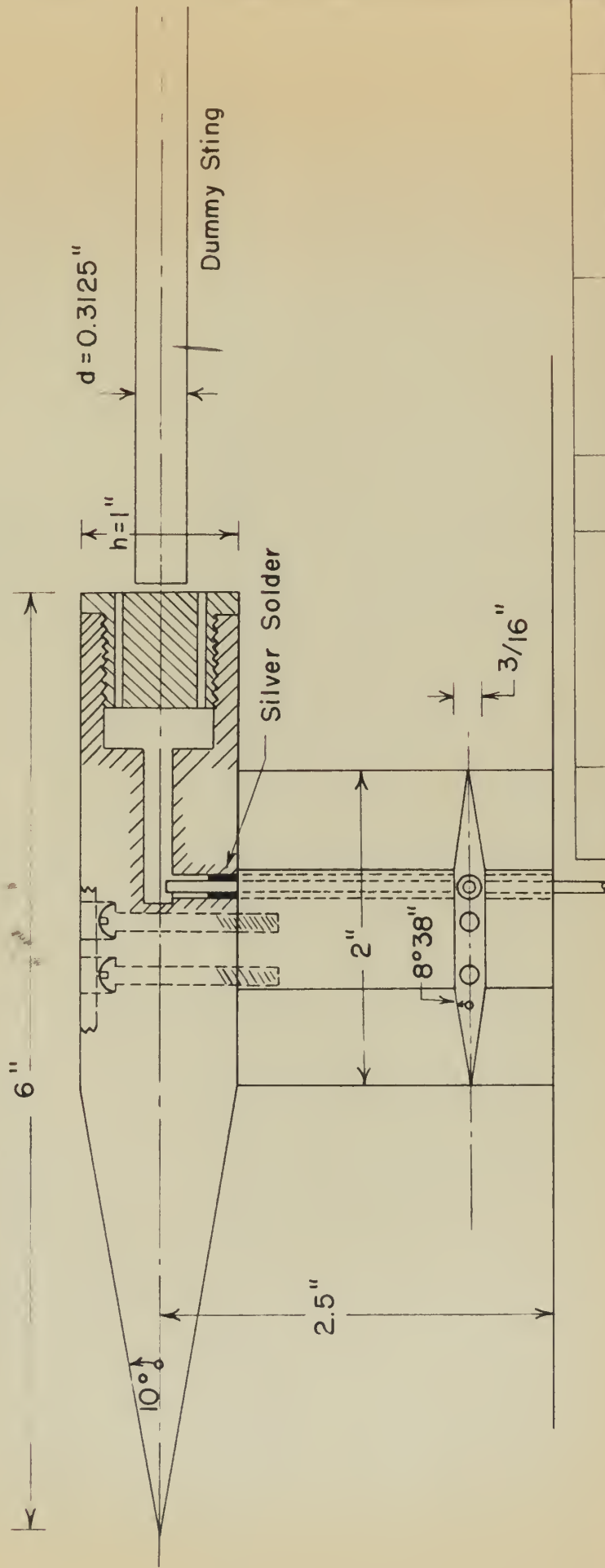
NUMBER	TITLE	PAGE
1	Sting-Supported Base Pressure Model	19
2	Side-Supported Base Pressure Model	20
3	Sting-Supported Static Pressure Model	21
4	Base Pressure Models with Shrouds	22
5	Static Pressure Model Showing Orifices	22
6	Sting-Supported Model in Hypersonic Tunnel	23
7	Side-Supported Model in Hypersonic Tunnel	23
8	Schlieren Photograph of Cone	24
9	Schlieren Photograph of Model Base and Sting	24
10	Effect of Varying Sting Length	25
11	Effect of Varying Sting Diameter	26
12	Base Pressure Coefficient Vs. Reynolds Number	27
13	Static Pressure Distribution	28





PART NO.		NAME		NO. REQ.		MATERIAL DESC.		MATERIAL SPEC.		WEIGHT	
CALIFORNIA INSTITUTE of TECHNOLOGY											
FIG. 1 - STING SUPPORTED BASE PRESSURE MODEL											
FINISH						DRAWN BY					
HEAT TREAT						TRACED BY					
						CHECKED BY					
						APPROVED BY					
						DATE					
						COURSE NO.					
						SECTION NO.					
						DWG. NO.					
						NO.					

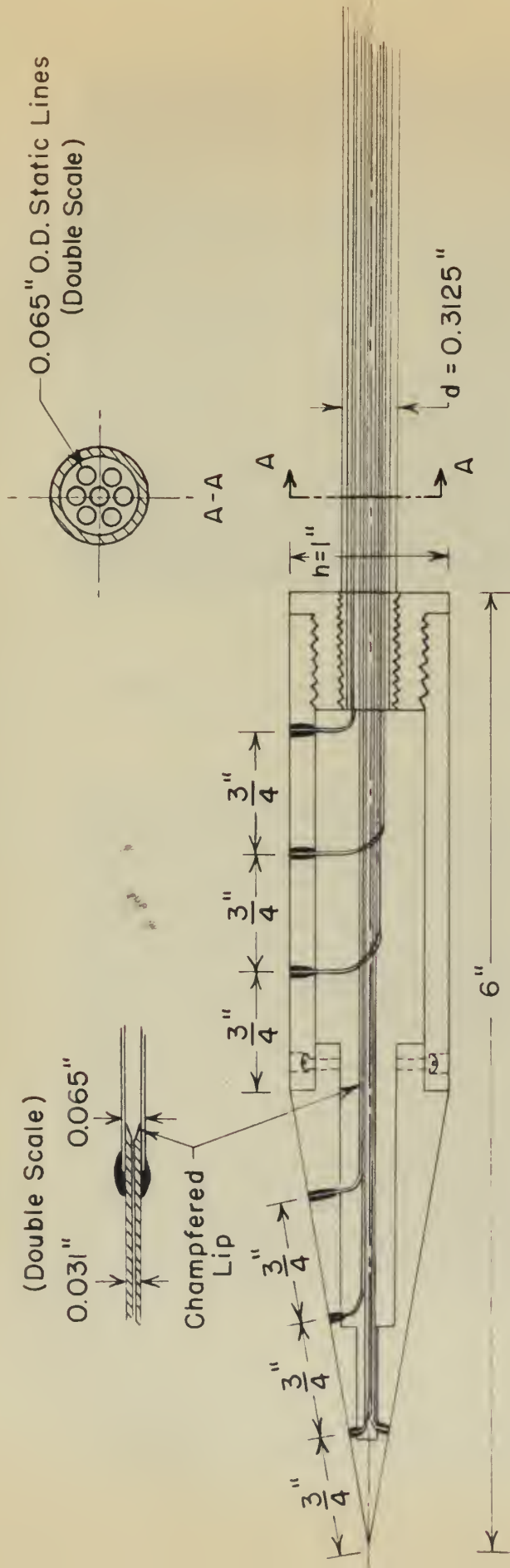




ALL DIMENSIONS IN INCHES LIMIT ON DIMENSIONS ——— UNLESS OTHERWISE NOTED		FINISH  HEAT TREAT		CALIFORNIA INSTITUTE OF TECHNOLOGY  FIG. 2 - SIDE SUPPORTED BASE PRESSURE MODEL				DRAWN BY TRACED BY CHECKED BY APPROVED BY		MATERIAL DESC. MATERIAL SPEC. WEIGHT	
ANGULAR $\pm \frac{1}{2}^\circ$ FRACTIONAL $\pm \frac{1}{32}$ DECIMAL $\pm .010$		NUMBERS ARE SURFACE ROUGHNESS IN MICROINCHES $\frac{1}{8}$ FINISH GRIND $\frac{2}{1250}$ FINE GRIND. LAP $\frac{1}{40}$ POLISH ROUGH GRIND		PART NO. NAME NO. QRD MATERIAL DESC.				COURSE NO. SECTION NO.		SCALE Full DWG NO.	







PART NO.		NAME		NO. REQ.		MATERIAL DESC.		MATERIAL SPEC.		WEIGHT	
CALIFORNIA INSTITUTE of TECHNOLOGY											
FIG. 3 - STING SUPPORTED STATIC PRESSURE MODEL											
FINISH		DRAWN BY		MATERIAL SPEC.		DATE		SCALE		Full	
HEAT TREAT		TRACED BY		COURSE NO.		DWG		NO			
CHECKED BY		SECTION NO.		APPROVED BY							
APPROVED BY											
DATE											
COURSE NO.											
SECTION NO.											





**FIGURE 4**      **BASE PRESSURE MODELS WITH SHROUDS**



**FIGURE 5**      **STATIC PRESSURE MODEL SHOWING ORIFICES**



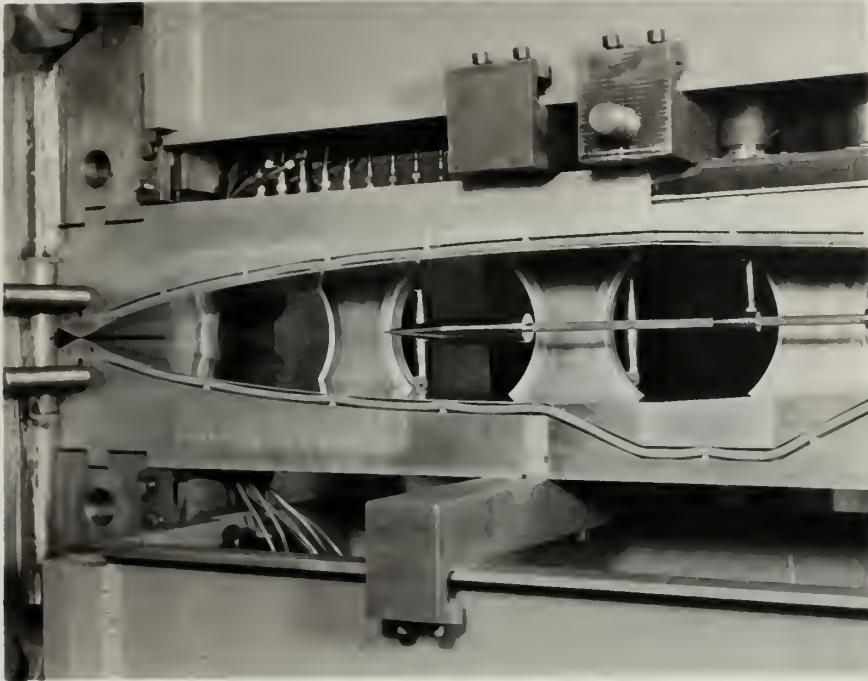


FIGURE 6

STING SUPPORTED MODEL IN HYPERSONIC TUNNEL

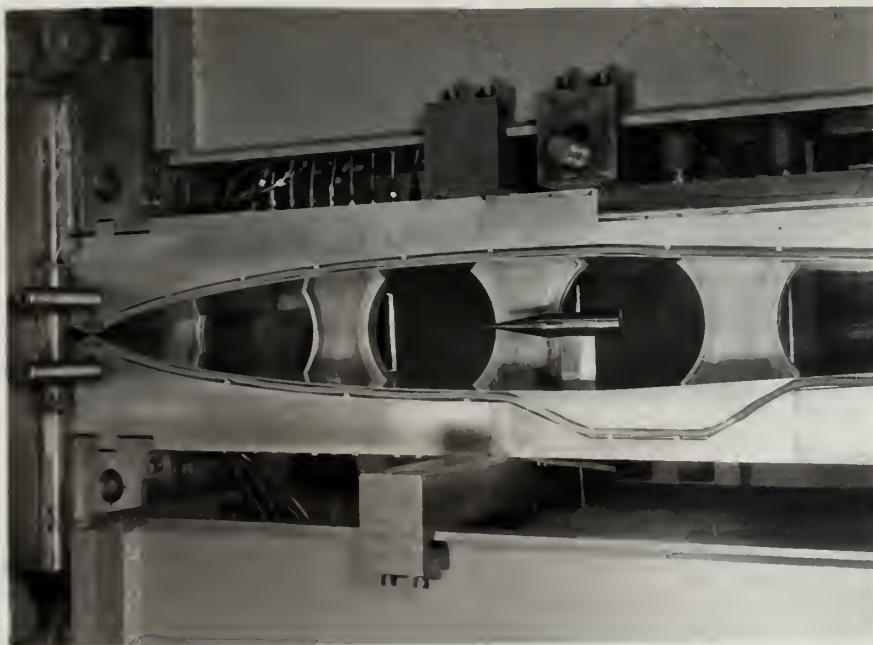


FIGURE 7

SIDE SUPPORTED MODEL IN HYPERSONIC TUNNEL





FIGURE 8

SCHLIEREN PHOTOGRAPH OF CONE



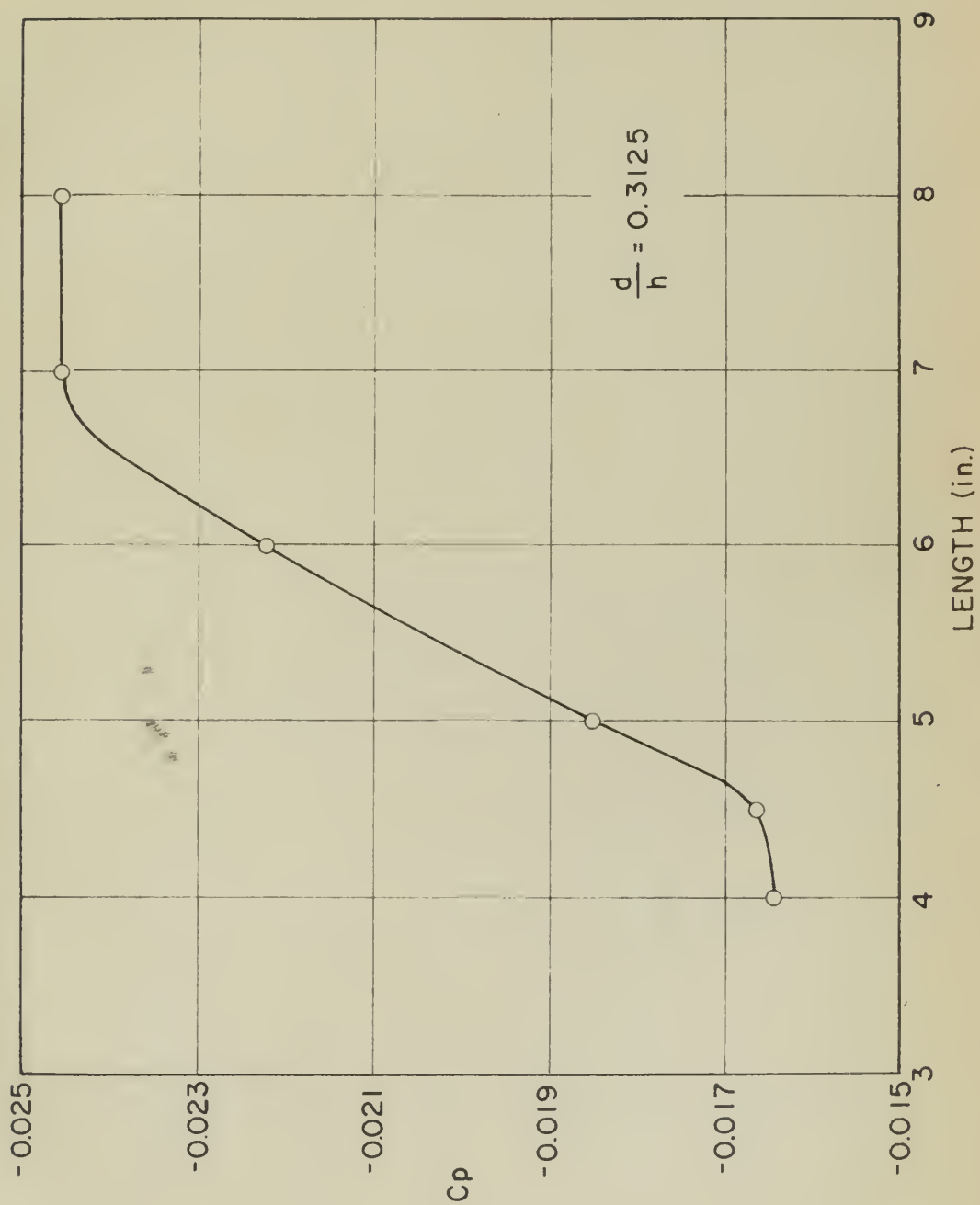
FIGURE 9

SCHLIEREN PHOTOGRAPH OF MODEL BASE AND STING SHOWING INTERFERENCE

$$(l/h = 4.1)$$

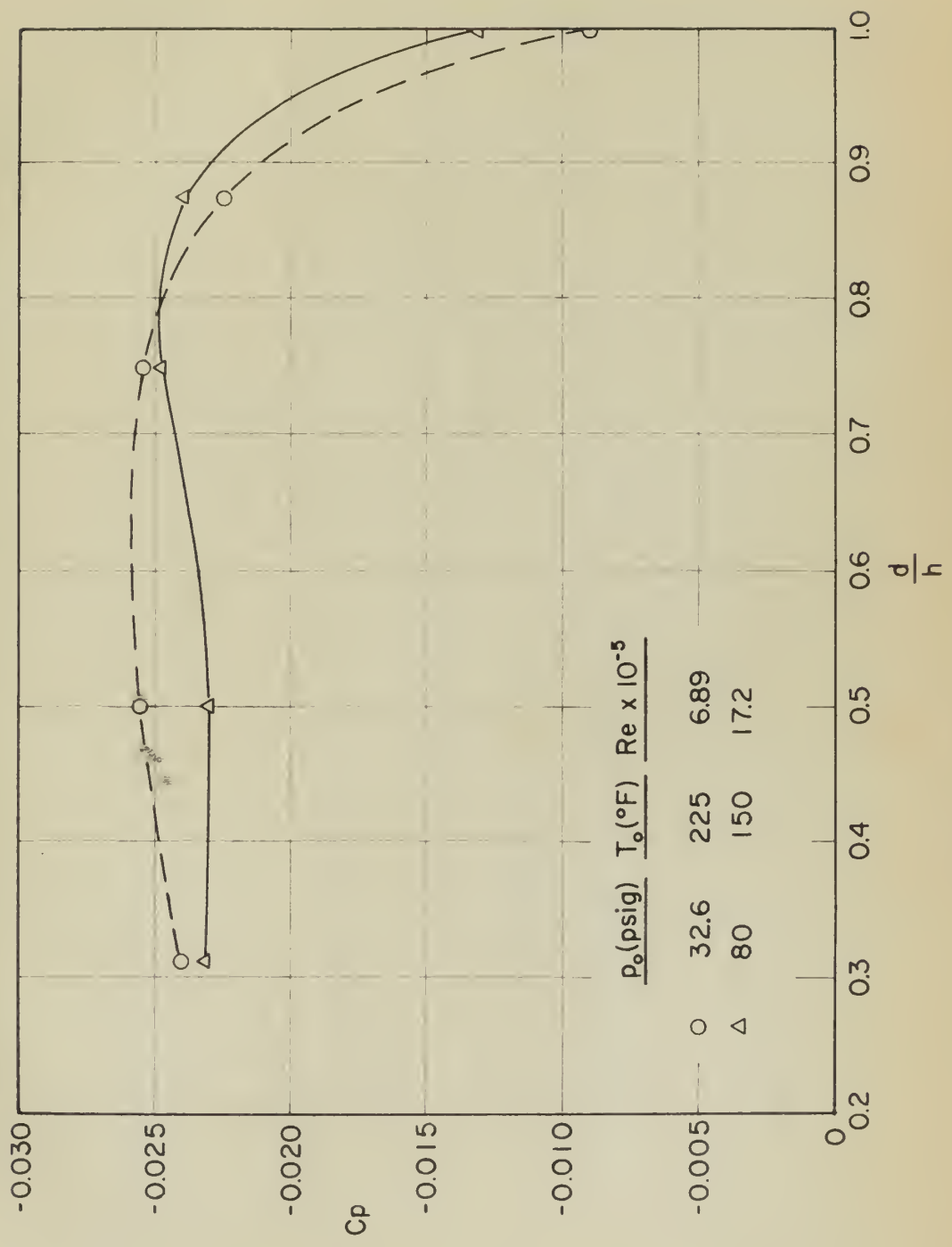






EFFECT OF VARYING STING LENGTH  
FIG. 10

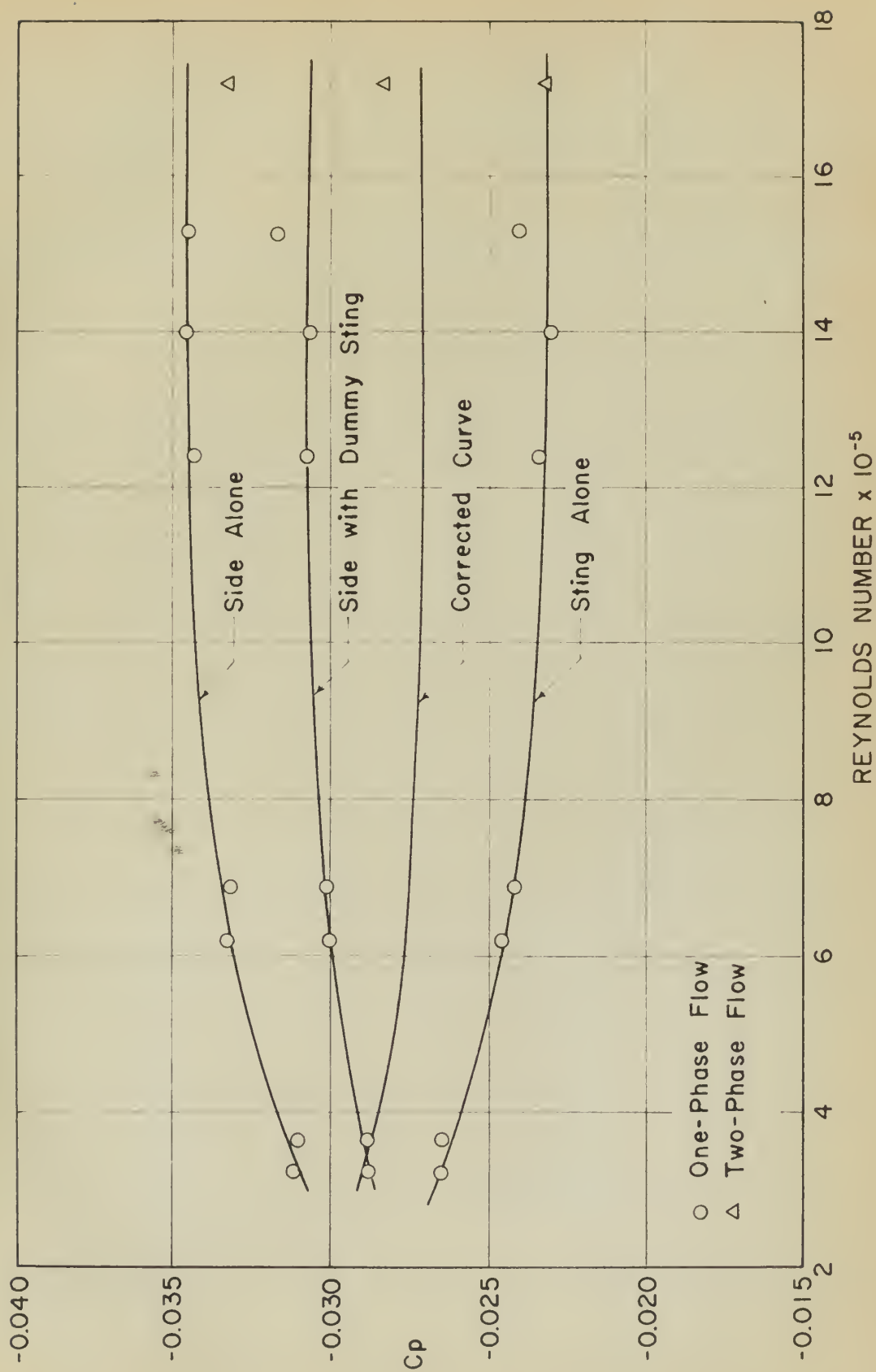




EFFECT OF VARYING STING DIAMETER

FIG. 11

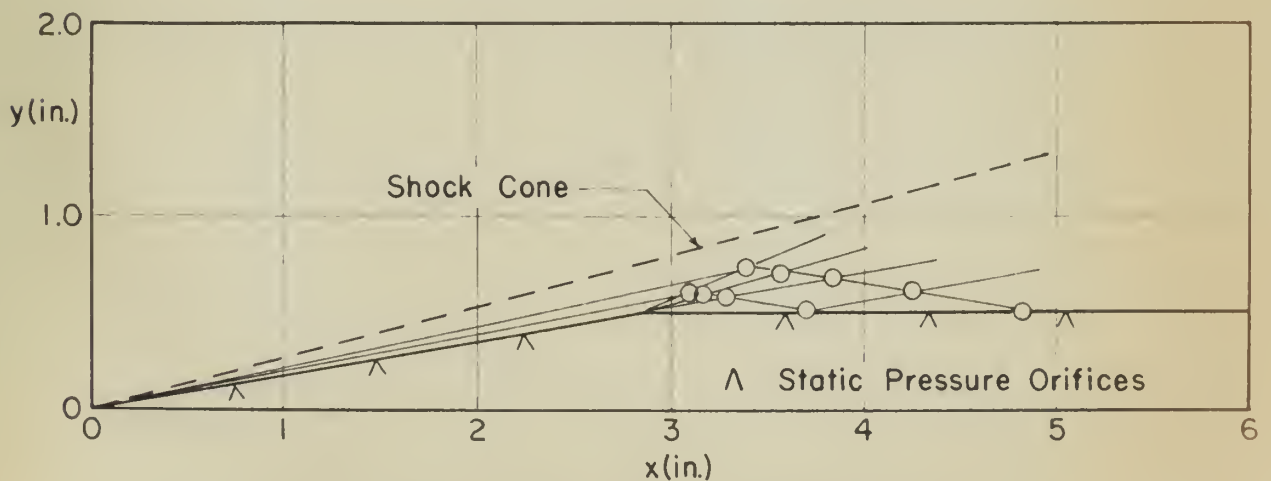
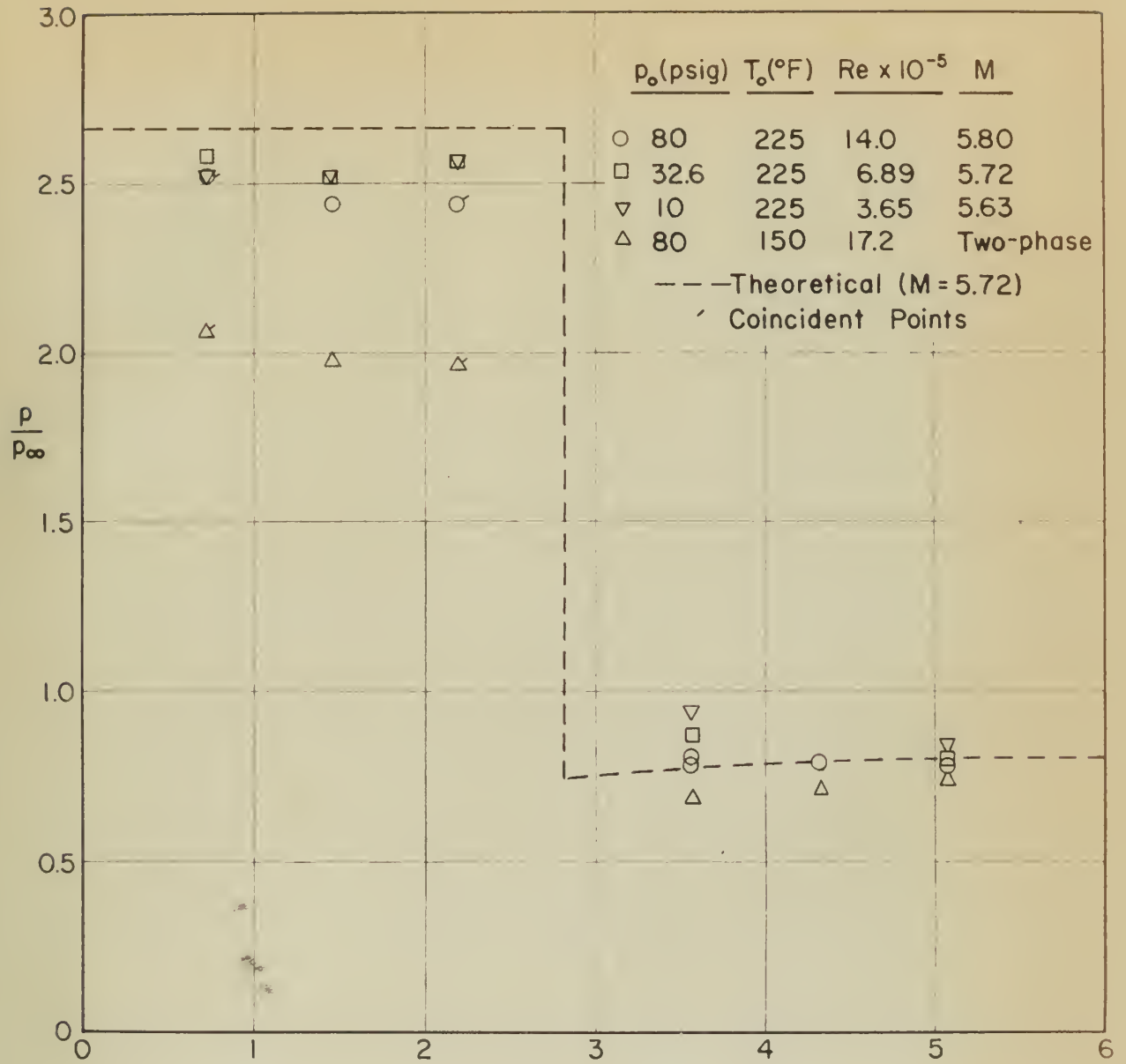




BASE PRESSURE COEFFICIENT VS. REYNOLDS NUMBER

FIG. 12





STATIC PRESSURE DISTRIBUTION

FIG. 13













Ther  
F23

Harkins

28831

Base pressure and static  
pressure for a cone-cylin-  
der at a nominal mach  
number of 5.8.

Ther  
F23

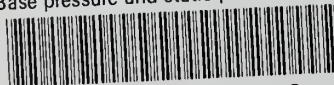
Harkins

28831

Base pressure and static pres-  
sure for a cone-cylinder at  
nominal mach number of 5.8.

thesH23

Base pressure and static pressure for a



3 2768 002 08183 8

DUDLEY KNOX LIBRARY